Dalton Transactions

PAPER

View Article Online
View Journal | View Issue

Cite this: *Dalton Trans.*, 2015, **44**, 14494

Ferrocenylmethylation reactions with a phosphinoferrocene betaine†

Martin Zábranský, Ivana Císařová and Petr Štěpnička*

A phosphinoferrocene betaine, *N*-{[1′-(diphenylphosphino)ferrocenyl]methyl}-*N*,*N*-dimethyl-3-sulfo-1-propanaminium, inner salt, $Ph_2PfcCH_2NMe_2(CH_2)_3SO_3$ (**2**; fc = ferrocene-1,1′-diyl), was prepared by alkylation of $Ph_2PfcCH_2NMe_2$ (**1**) with 1,3-propanesultone, and was studied as a ferrocenylmethylation agent. The treatment of **2** with NaOH in hot water–dimethyl sulfoxide produced phosphinoalcohol Ph_2PfcCH_2OH (**3**) in a 64% yield, whereas a similar reaction with MeONa in dimethylsulfoxide–methanol furnished the corresponding ether, Ph_2PfcCH_2OMe (**4**), in a 47% yield. In subsequent experiments, betaine **2** was employed in the synthesis of phosphinoferrocene sulfones, $Ph_2PfcCH_2SO_2R$, where R = Me (**6a**), Ph (**6b**), and 4-tolyl (**6c**). Compounds **6a–c** and some by-products of the ferrocenylmethylation reactions, namely alcohol **3**, 1′-(diphenylphosphino)-1-methylferrocene (**5**), and 1-{[diphenyl(2,4-cyclopentadien-1-ylidene)phosphoranyl]methyl}-1′-(diphenylphosphino)ferrocene (**7**) structurally characterised. Reactions of **6a** as the representative with ZnX_2/NaX (X = Br and I) afforded unique coordination polymers $[ZnNaX_3(\mathbf{6a})(CH_3OH)]_n$ featuring tetrahedral Zn(II) and octahedral Na(I) centres bridged by halide ions, solvating methanol and the sulfone ligands. The reaction of **6a** with $ZnBr_2$/KBr produced an analogous product, $[ZnKBr_3(\mathbf{6a})(CH_3OH)]_n$, while that with $ZnBr_2$/LiBr furnished a different, pseudodimeric complex $[Zn_2Li_2Br_6(\mathbf{6a})_2(CH_3OH)_4(H_2O)]\cdot CH_3OH$, featuring tetrahedrally coordinated Zn(II) and Li(I) centres bridged by **6a**. Reactions of **6a** with $ZnBr_2$/MBr (M = Rb, Cs) and NaCl/$ZnCl_2$ did not yield similar products because of an easy precipitation (low solubility) of the respective alkali metal halides.

Received 19th May 2015,
Accepted 7th July 2015

DOI: 10.1039/c5dt01877c

www.rsc.org/dalton

Introduction

Shortly after the discovery of ferrocene[1] and the elucidation of its real structure[2] in the early 1950s, ferrocenylmethylation was recognised as a powerful method for the preparation of various ferrocene derivatives.[3] This reaction typically utilises stable starting materials capable of serving as precursors of the stabilised ferrocenylmethylium cation,[4] which is allowed to react with nucleophiles (Nu) to afford derivatives of the type $FcCH_2Nu$ (Fc = ferrocenyl). The most often employed ferrocenylmethylation reagents are undoubtedly $FcCH_2NMe_2$ and $[FcCH_2NMe_3]I$, with which the reaction was developed, though other compounds, *e.g.*, $[FcCH_2PPh_3]I$ or $FcCH_2OH$ (the latter in combination with an acid), have also found practical applications.[3]

In the synthesis of phosphinoferrocene donors,[5] ferrocenylmethylation reactions have been applied only rarely because of competitive reactions affecting the phosphine moieties (alkylation).[6] Therefore, the [1′-(diphenylphosphino)ferrocene-1-yl]-methyl derivatives have typically been synthesised either indirectly (*e.g.*, *via* late-stage lithiation/phosphinylation[7]) or from P-protected building blocks, such as $Ph_2P(S)fcCH_2OH$[8] or the borane adduct $Ph_2PfcCH_2OH\cdot BH_3$.[9]

In view of our recent work focusing on the preparation and coordination properties of 1′-(diphenylphosphino)-1-[(dimethylamino)methyl]ferrocene (**1**)[10,11] and other 1′-functionalised phosphinoferrocene derivatives possessing an inserted methylene group,[9,12] we wanted to extend the hitherto unexplored synthetic chemistry of the former compound, which led us to attempt the preparation of ammonium salts derived from **1** and study their prospective synthetic applications. In this contribution, we describe the selective synthesis and structural characterisation of the phosphinoferrocene betaine $Ph_2PfcCH_2N^+Me_2(CH_2)_3SO_3^-$ (**2**; fc = ferrocene-1,1′-diyl) and its utilisation in the preparation of the known and some new 1′-functionalised phosphinoferrocene donors such as 1′-[(diphenylphosphino)ferrocenyl]methyl sulfones $Ph_2PfcCH_2SO_2R$. Furthermore, we report on the reactions of the representative ligand, $Ph_2PfcCH_2SO_2Me$, with zinc(II) and alkali metal

---

Department of Inorganic Chemistry, Faculty of Science, Charles University in Prague, Hlavova 2030, 128 40 Prague, Czech Republic. E-mail: stepnic@natur.cuni.cz

† Electronic supplementary information (ESI) available: A comparison of the IR spectra of **6a**, **8a**, and **8b** in the fingerprint region, additional structural drawings for **8a** and **8b**, and a summary of the crystallographic data and structure refinement parameters (Table S1). CCDC 1401233–1401241, 1410159 and 1410160. For ESI and crystallographic data in CIF or other electronic format see DOI: 10.1039/c5dt01877c

halides, leading to structurally unique mixed-metal coordination polymers.

Results and discussion

Synthesis of betaine 2 and initial reaction tests

Betaine **2** was synthesised similarly to its non-phosphinylated analogue (Scheme 1)[13] by the reaction of phosphinoamine **1**[10] with 1,3-propanesultone (1,2-oxathiolane-2,2-dioxide) in dry benzene. The compound was isolated by column chromatography, resulting as an air-stable orange solid in an 81% yield (at the 10 mmol scale).[14] Crystallisation from methanol–tetrahydrofuran–diethyl ether afforded the stoichiometric solvate **2**·CH_3OH, which was structurally characterised by single-crystal X-ray diffraction analysis (*vide infra*).

The ^1H and ^{13}C NMR spectra of **2** combine the signals due to the phosphinoferrocenyl moiety with those of the NMe_2 group and the propane-1,3-diyl bridge. The ^{31}P NMR resonance is observed at δ_P −18.1 ppm, suggesting that the phosphine moiety remained intact. In its IR spectrum, betaine **2** shows strong signals attributable to the vibrations of the terminal sulfonate moiety (ν_s 1037 cm^{-1} and ν_{as} 1189 cm^{-1}), whereas the electrospray ionisation (ESI) mass spectrum reveals signals of the pseudomolecular ions $[M + X]^+$, where M = H, Na, and K, and of the characteristic fragment[15] ions due to the substituted ferrocenylmethylium cation $[Ph_2PfcCH_2]^+$ at *m*/*z* 383.

The possible synthetic applications of betaine **2** were first examined by its conversion into the known alcohol **3**[12a] and the corresponding methyl ether **4**[9] *via* reactions with the respective nucleophiles (Scheme 1). These ferrocenylmethylation reactions were carried out similarly to the literature[13,16] but carefully optimised. For solubility reasons, dimethyl sulfoxide was chosen as the solvent, and the reactions were performed at temperatures above 100 °C since lower reaction temperatures markedly reduced the yield of the substitution product (N.B. unreacted **2** could be recovered from the reaction mixture in such cases). The reaction time was maintained at minimum (typically 1 h) in order to prevent decomposition and oxidation of the phosphine moiety.

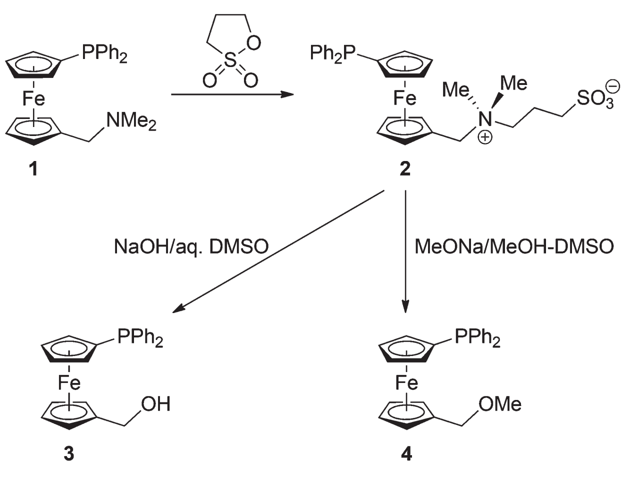

Scheme 1 Synthesis and model reactions of betaine **2**.

For the preparation of alcohol **3**, the best reaction conditions were found to consist of refluxing the solution of betaine **2** in a mixture of DMSO and 2 M aqueous NaOH (1 : 1; the concentration of NaOH in the resulting solution was 1 M) for 1 h. Product **3** was isolated by extraction and purified by column chromatography, resulting in a 64% yield (at the 2 mmol scale). A small amount of a less polar side-product was also isolated, being identified as 1′-(diphenylphosphino)-1-methyl-ferrocene, Ph_2PfcMe (**5**; typically *ca.* 5%). This rather unexpected product probably results *via* "quenching" of the intermediate cation $Ph_2PfcCH_2^+$ upon attack of other C–H bonds (acid–base equilibria) rather than by interaction with any proton source in the reaction system.

The etherification reaction was similarly performed in a mixture of dimethyl sulfoxide and methanolic MeONa (1 M MeONa in the reaction system) at lower temperatures (but still under reflux conditions) for 2 h, affording phosphinoether **4** in a 47% isolated yield.

The crystal structures of 2·CH_3OH and 5

The solvate **2**·CH_3OH, isolated after crystallisation by liquid-phase diffusion of tetrahydrofuran and diethyl ether into a solution of the betaine in methanol, crystallises with the symmetry of the triclinic space group $P\bar{1}$. Its structure is presented in Fig. 1, and the relevant geometric data are summarised in Table 1.

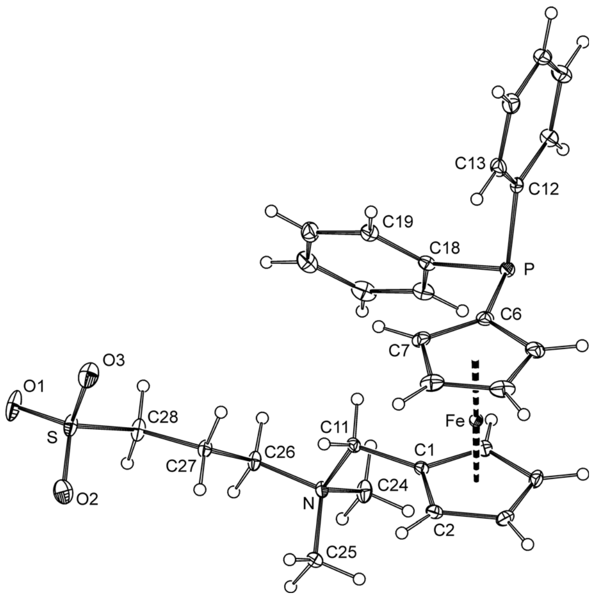

Fig. 1 PLATON plot of the phosphinobetaine molecule in the structure of **2**·CH_3OH showing the atom-labelling scheme and displacement ellipsoids at a 30% probability level.

Table 1 Selected interatomic distances and angles for **2**·CH_3OH (in Å and °)[a]

Distances		Angles	
S–O1	1.463(1)	C6–P–C12	102.25(6)
S–O2	1.450(1)	C6–P–C18	101.92(6)
S–O3	1.454(1)	C12–P–C18	102.45(6)
S–C28	1.777(2)	O1–S–O2	112.85(7)
N–C11	1.525(2)	O1–S–O3	113.21(7)
N–C24	1.499(2)	O2–S–O3	113.00(7)
N–C25	1.497(2)	C28–S–O1	103.67(7)
N–C26	1.518(2)	C28–S–O2	106.38(7)
P–C6	1.811(1)	C28–S–O3	106.84(7)
P–C12	1.834(1)	C1–C11–N–C26	−177.8(1)
P–C18	1.837(1)	C11–N–C26–C27	−54.8(1)
C1–C11	1.489(2)	N–C26–C27–C28	−172.0(1)
C1S–O1S	1.412(2)	C26–C27–C28–S	171.39(9)

[a] Note: parameters pertaining to the ferrocene moiety as well as the N–C–N angles are discussed in the main text.

The ferrocene unit in the structure of **2** shows similar Fe–C distances (2.019(1)–2.051(1) Å) and, accordingly, practically negligible tilting (the dihedral angle of the least-squares planes of the cyclopentadienyl ring is 1.40(8)°). The substituents attached to the ferrocene moiety adopt a nearly ideal synclinal eclipsed conformation, as evidenced by the torsion angle C1–Cg1–Cg2–C6 of −73.49(9)° (*cf.* the ideal value of 72°).

The carbons surrounding the positively charged nitrogen atom in **2** constitute a regular tetrahedral environment, with the C–N distances and associated bond angles (C–N–C) in the range of 1.497(2)–1.525(2) Å and 106.9(1)–111.0(1)°, respectively. The environment of the sulfur atom is somewhat distorted, presumably because of the different sizes of the bonded atoms and, also, a repulsion of the oxygen atoms (S–C > S═O and O═S═O > C–S═O; see parameters in Table 1).

The individual molecules constituting the crystals of **2**·CH_3OH assemble into dimers of inversion-related molecules through charge-supported hydrogen bonds between two oxygen atoms of the negatively charged sulfonate group and the CH_3 hydrogens polarised by the positively charged nitrogen (Fig. 2). The solvating methanol forms an O–H⋯O hydrogen bond with the remaining sulfonate oxygen. Additional C–H⋯O interactions further interconnect the $(\mathbf{2})_2(CH_3OH)_2$ units into columnar stacks oriented along the crystallographic *a*-axis.

The solid-state structure of **5** (Fig. 3) resembles that of the corresponding borane adduct **5**·BH_3.[9] Whereas the C1–C11 bond lengths (1.497(2) Å) in both compounds are practically identical (within the three-sigma level), the P–C bonds in **5** (P–C6 1.810(2), P–C12 1.841(2), and P–C18 1.834(2) Å) are slightly but statistically significantly longer (by *ca.* 0.02 Å) than those in the mentioned reference compound, reflecting the electronic changes associated with the adduct formation ($R_3P \rightarrow BH_3$). The Fe–C distances in the molecule of **5** span a narrow range of 2.037(1)–2.051(2) Å, which is in turn reflected in an insignificant tilting of the cyclopentadienyl rings (the tilt angle is as low as 1.1(1)°). As indicated by the torsion angle C1–Cg1–Cg2–C6 of −77.8(1)°, the ferrocene unit has a synclinal eclipsed conformation, which is also similar to that of the aforementioned borane adduct.

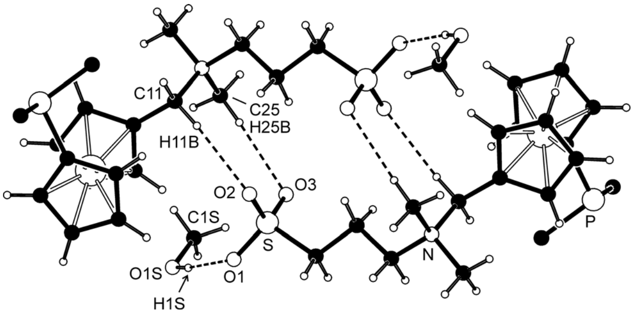

Fig. 2 View of the hydrogen bonded dimers in the structure of **2**·CH_3OH. For clarity, only the pivotal atoms of the phenyl rings are shown. The hydrogen bond parameters are as follows: C11–H11B⋯O2^i: C11⋯O2 = 3.417(2) Å, angle at H11 = 166°; C25–H25B⋯O3^i: C25⋯O3 = 3.396(2) Å, angle at H25B = 167°; O1S–H1S⋯O1: O1S⋯O1 = 2.719(2) Å, angle at H1S = 172°; (i) (1 − *x*, 1 − *y*, 2 − *z*).

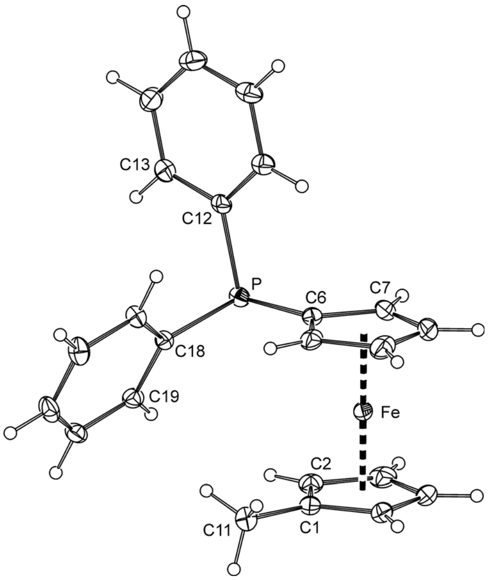

Fig. 3 PLATON plot of the molecular structure of **5** showing 30% displacement ellipsoids.

Synthesis and characterisation of phosphine-sulfones 6

Aiming at the preparation of *new* phosphinoferrocene ligands *via* ferrocenylmethylation, betaine **2** was subsequently reacted with sodium sulfinates to give the respective phosphino-ferrocene sulfones **6** (Scheme 2). The reactions were performed with an excess of the sulfinate salts (**2** : RSO_2Na = 1 : 2.5) in refluxing DMSO–water for 2 h, similarly to the synthesis of ferrocenylmethyl sulfones $FcCH_2SO_2R$ from simple ferrocenylmethylation agents.[13,17]

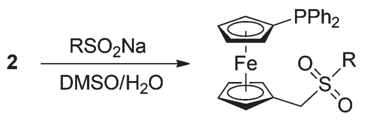

6a (R = Me)
6b (R = Ph)
6c (R = C_6H_4Me-4)

Scheme 2 Preparation of phosphinoferrocenyl sulfones **6**.

The yields of the sulfones after chromatographic purification were *ca.* 30% for **6a** and approximately 50% for the compounds bearing the aromatic substituents (**6b** and **6c**), which are less than in the reactions leading to $FcSO_2R$. Therefore, we sought for other reaction products to gain more detailed information regarding the course of these particular ferrocenylmethylation reactions.

In the case of the reaction of betaine **2** with $MeSO_2Na$, a careful chromatographic purification of the reaction mixture led to the isolation of alcohol **3** (2%) and phosphorane **7** (Scheme 3; 12%). Together with **6a**, compounds **3** and **7** account for nearly 45% of the starting material. The reactions leading to aryl sulfones **6b** and **6c** are more selective (isolated yields: *ca.* 50%) but afford identical by-products (isolated yields of **3** and **7** are *ca.* 3% and 10–15%, respectively). Apparently, the cation $Ph_2PfcCH_2^+$ generated *in situ* from **2** enters into reactions with all other available nucleophiles, including OH^- or phosphines. Interaction with the latter provides cationic products (*i.e.*, phosphonium salts arising from “self-alkylation” of the parent **2** with $Ph_2PfcCH_2^+$) and, consequently, also their decomposition products such as **7**. The fact that no **7** could be detected in the reaction mixtures obtained after treatment of **2** with NaOH and NaOMe (*vide supra*) can well reflect the higher relative amounts of these nucleophilic reagents, that suppress the competing reactions with other nucleophiles. Attempts to isolate the anticipated cationic (and hence more polar) side products or to recover unreacted **2** during the course of chromatographic purification of crude sulfones **6** failed.

The formulation of **6a–c** and **7** was inferred from NMR and IR spectra, ESI mass spectra, and elemental analysis and was unequivocally confirmed by single-crystal X-ray diffraction. The NMR spectra of sulfones **6** comprise the signals due to the (diphenylphosphino)ferrocenyl unit and its attached methylene linker (CH_2: δ_H/δ_C 3.59/56.65 for **6a**, and *ca.* 3.68/58.3 for **6b** and **6c**). The signals of the sulfone substituents, as well as the ^{31}P NMR resonances ($\delta_P \approx -17$ ppm), are observed in the usual ranges. The IR spectra of the sulfones display the characteristic strong bands of the sulfone moieties centred at approximately 1310 (ν_{as}) and 1145 cm^{-1} (ν_s).[17a]

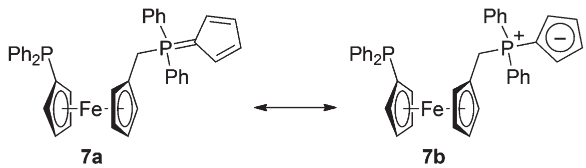

7a **7b**

Scheme 3 Canonical forms of compound **7**.

The ^1H and ^{13}C NMR spectra of the by-product **7** contain signals of the 1,1′-disubstituted ferrocene moiety and two sets of resonances of the non-equivalent PPh_2 groups, which is also reflected in the ^{31}P NMR spectrum showing two singlets at δ_P −16.9 and 10.1. The presence of the cyclopentadienylidene unit[18] in **7** is manifested by a pair of multiplets at δ_H 6.12 and 6.40 and a pair of doublets at δ_C 113.92 and 115.83 in the ^1H and ^{13}C NMR spectra, respectively. The ^{13}C NMR signal due to C_{ipso} in the $P{=}C_5H_4$ moiety is observed at δ_C 78.21 as a phosphorus-coupled doublet ($^1J_{PC}$ = 110 Hz). The signals of the connecting methylene group are found at δ_H 3.59 (doublet with $^2J_{PH}$ = 12.7 Hz) and δ_C 30.01 (dd, $^1J_{PC} = 53, J_{PC} = 1$ Hz).

Crystallisation of **6a** from ethyl acetate–hexane provided crystals of a triclinic modification (denoted as **6a**). Crystals of another polymorph, **6a′**, were serendipitously isolated during an attempted preparation of Zn(II) complexes, *i.e.*, upon crystallization of a **6a**/$ZnBr_2$ mixture from methanol–diethyl ether (*vide infra*). The polymorphs differ by the symmetry of the crystal lattice (**6a**: triclinic, $P\bar{1}$; **6a′**: monoclinic, $P2_1/c$) and by the overall conformation of the molecules constituting their crystals (Fig. 4 and Table 2).

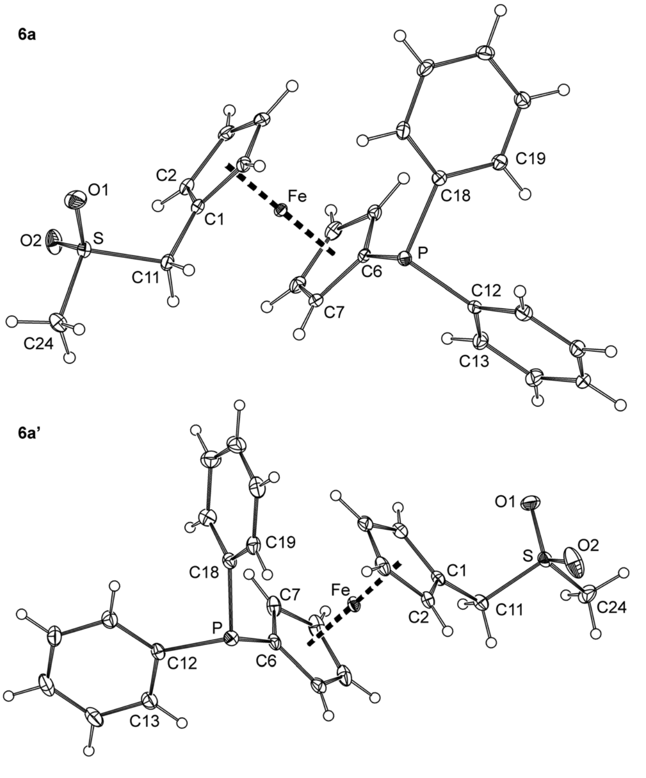

Fig. 4 PLATON plots of the molecular structures of the triclinic (top; **6a**) and monoclinic (bottom; **6a′**) polymorphs of 1′-(diphenylphosphino)-1-[(methylsulfonyl)methyl]ferrocene. The displacement ellipsoids enclose the 30% probability level.

Table 2 Selected geometric parameters of the molecules of phosphinosulfones **6** (in Å and °)

Parameter[a]	6a	6a′	6b	6c
Fe–C	2.031(2)–2.060(2)	2.035(2)–2.054(2)	2.026(1)–2.058(2)	2.040(2)–2.056(2)
Tilt	2.98(9)	3.3(1)	2.64(9)	1.9(1)
C1–Cg2–Cg2–C6	−79.1(1)	162.5(1)	128.2(1)	73.3(1)
P–C6	1.817(2)	1.821(2)	1.812(2)	1.815(2)
P–C12	1.838(2)	1.835(2)	1.832(2)	1.835(2)
P–C18	1.839(2)	1.832(2)	1.834(2)	1.834(2)
C1–C11	1.494(2)	1.494(3)	1.488(2)	1.489(3)
C11–S	1.786(2)	1.781(2)	1.784(2)	1.792(2)
S–O1	1.435(1)	1.432(2)	1.446(1)	1.440(2)
S–O2	1.439(1)	1.433(2)	1.441(1)	1.445(2)
S–C24	1.764(2)	1.754(2)	1.765(2)	1.770(2)
C1–C11–S	111.5(1)	110.9(1)	113.0(1)	111.8(1)
O1–S–O2	117.80(8)	117.6(1)	118.60(7)	118.42(9)
C11–S–C24	103.23(7)	103.2(1)	103.72(7)	106.67(8)
C1–C11–S–C24	176.3(1)	−178.6(1)	−55.3(1)	71.8(1)

[a] Definitions: tilt stands for the dihedral angle of the least-squares planes of the cyclopentadienyl rings. The torsion angle C1–Cg2–Cg2–C6 reflects the mutual conformation of the substituents at the ferrocene unit; Cg1 and Cg2 are the centroids of the cyclopentadienyl rings C(1–5) and C(6–10), respectively.

Thus, whereas the molecular structures of the two polymorphs are expectedly very similar in terms of interatomic distances and angles, they differ in the mutual orientation of the substituted cyclopentadienyl rings, which are nearly synclinal eclipsed in **6a** and exactly halfway between anticlinal eclipsed and antiperiplanar staggered in **6a′** (compare the C1–Cg1–Cg2–C6 angles in Table 1).[19] Another less pronounced difference can be observed in the orientation of the PPh_2 units resulting from different rotations along the pivotal C6–P bond and from the tilting of the phenyl rings.

The geometry of the (methylsulfonyl)methyl moiety in **6a** and **6a′** agrees well with that of, *e.g.*, phenyl methyl sulfone, 4-methoxyphenyl methyl sulfone,[20] and (benzylsulfonyl)methanol.[21] Similar to these compounds, the O1–S–O2 angle is the most opened and the C11–S–C24 angle is the most acute among the bond angles around the sulfur atoms in **6a** and **6a′**, most likely due to an electrostatic repulsion of the electronegative oxygen atoms.

The main difference between the molecular structures of sulfones **6b** and **6c** (Fig. 5 and Table 2) can also be found in the conformation of the 1,1′-disubstituted ferrocene unit, which is intermediate between anticlinal staggered and anticlinal eclipsed for **6b** and synclinal eclipsed for **6c**. In both cases, the CH_2SO_2Ar (Ar is an aryl) pendants extend away from the ferrocene core but adopt different orientations as indicated by the torsion angle C1–C11–S–C24 (see Table 2) and the dihedral angles of the C(1–5) and C(24–29) ring planes of 45.93(8)° and 33.5(1)° for **6b** and **6c**, respectively. On the other hand, the compounds comprise regular ferrocene moieties (tilt angles below *ca.* 3°) and show similar individual interatomic distances and angles that do not depart substantially from those of **6a**/**6a′** and benzylsulfones of the type $ArCH_2SO_2Ar$ (Ar = an aryl).[22]

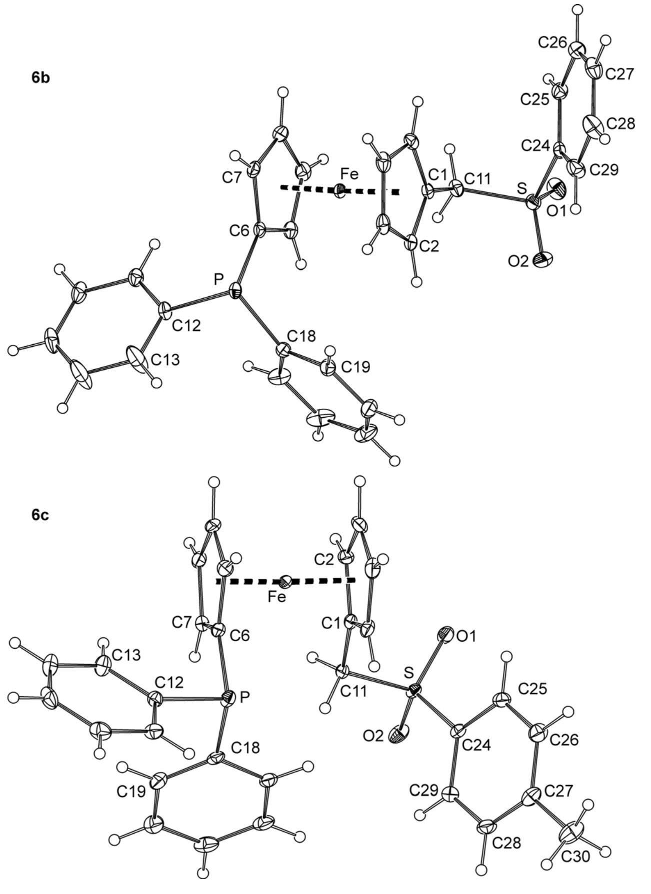

Fig. 5 PLATON plots of the molecular structure of the phosphinoferrocene sulfones **6b** and **6c** at the 30% probability level.

The ferrocene cyclopentadienyls in the structure of by-product **7** (Fig. 6) are tilted by 2.6(1)° and assume a conformation near synclinal eclipsed, as evidenced by the C1–Cg1–Cg2–C6 torsion angle of 79.3(1)°. The individual Fe–C distances are in the range of 2.026(2)–2.050(2) Å. The cyclopenta-

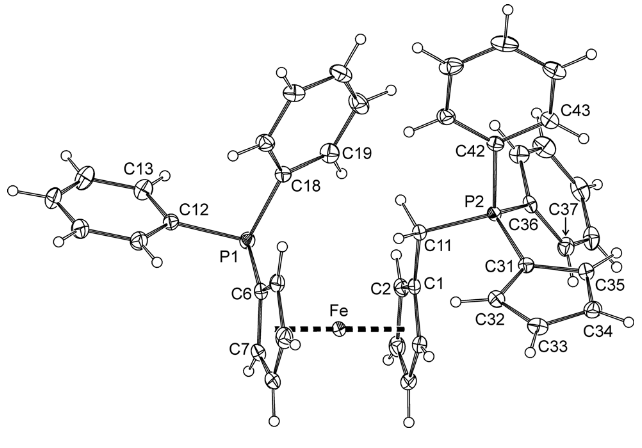

Fig. 6 PLATON plot of the molecular structure of **7** (30% displacement ellipsoids).

dienylidene substituent at the phosphorus P2 exhibits only moderate bond alternation (C31–C32 1.425(3), C32–C33 1.382(3), C33–C34 1.406(3), C34–C35 1.382(3), and C35–C31 1.414(3) Å). Its pivotal P2–C31 bond (1.722(2) Å) is of similar length to those in $MePh_2P{=}C_5R_4$ (R = H: 1.728(2) and 1.727(2) Å;[18] R = Me: 1.720(2) and 1.717(2) Å[23]). As such, it is shorter than the P1–C6 bond in **7** (1.811(2) Å) and the $P^+–C_5H_4$ bond in $[Fe(\eta^5\text{-}C_5H_4P^+Ph_2Me)\{\eta^5\text{-}C_5H_4Cr^-(CO)_6\}]$ (1.769(5) Å)[24] but longer than the $P{=}CH_2$ bond in the archetypal phosphorane $Ph_3P{=}CH_2$ (1.662(8) and 1.659(8) Å).[25] These features suggest compound **7** to possess an intermediate structure between two extreme canonical forms, *viz.* cyclopenta-2,4-dien-1-ylidene phosphorane (**7a**) and zwitterionic phosphonium cyclopentadienide (**7b**), as depicted in Scheme 3. It is also noteworthy that the P–Ph bonds are significantly longer for P1 (P1–C12 1.839(2), P1–C18 1.841(2) Å) than for P2 (P2–C36 1.801(2), P2–C42 1.810(2) Å), which bears a positive charge, most likely due to an electron density transfer from the aromatic rings to the partly positively charged P2. In contrast, the length of the P2–C11 bond (1.817(2) Å) agrees well with that of the similar bond in the phosphonium salt $[FcPPh_2(CH_2Ph)]Cl$ (1.819(3) Å).[26]

Preparation and structure of mixed-cation complexes with 6a

Coordination preferences of the newly prepared phosphinoferrocene sulfones were studied in reactions of **6a** as the model representative, with zinc(II) halides. These salts were chosen mainly due to the position of the Zn(II) ion at the borderline between hard and soft metal ions[27] and due to its closed (d^{10}) coordination sphere, which makes it structurally variable because of the absence of crystal-field stabilisation.[28]

To our disappointment, repeated experiments aiming at the preparation of defined products by co-crystallisation of zinc(II) halides with **6a** were unsuccessful. In one case, the crystallisation of a $ZnBr_2$-**6a** mixture in methanol/diethyl ether provided crystals of monoclinic **6a′**. Eventually, the attempted preparation of a Zn(II) complex by reacting $ZnBr_2$ and **6a** at a 1 : 1 molar ratio in methanol–chloroform, followed by evaporation and crystallisation from $CHCl_3$/methyl *tert*-butyl ether, yielded a few crystals of **8b**, which were used directly for X-ray structure determination.[29] The intriguing structure of this rather unexpected product (*vide infra*) led us to study the formation of such complexes systematically by changing the halide in ZnX_2/NaX (NaCl–NaBr–NaI) and then also the alkali metal cation in $ZnBr_2$/MBr (M = Li, Na, K, Rb, and Cs).

Attempts to isolate any mixed-cation compound from the **6a**/$ZnCl_2$/NaCl system failed, presumably because of the ionic nature of NaCl, which limits its solubility in organic solvents. The experiments furnished only crystals of uncoordinated **6a**. On the other hand, the reactions of **6a** with NaX/ZnX_2, where X = Br and I (all in equimolar amounts), in methanol followed by crystallisation upon layering the reaction mixture with methyl *tert*-butyl ether produced the respective coordination polymers **8a** (X = Br) and **8b** (X = I) as orange, nicely crystalline, and air-stable solids in good yields (Scheme 4).

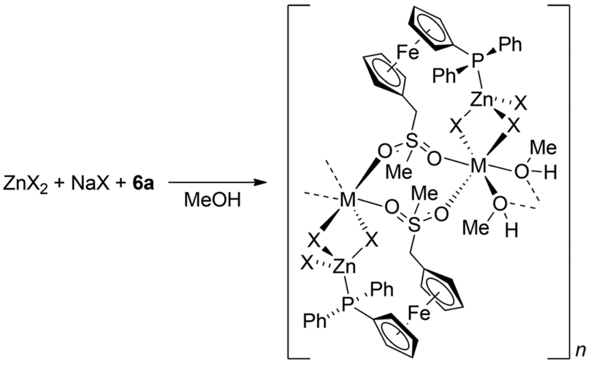

8a M = Na, X = Br
8b M = Na, X = I
9a M = K, X = Br

Scheme 4 Preparation of the mixed-metal complexes **8a**, **8b** and **9a**.

The reactions of **6a** with $ZnBr_2$ with other alkali metal bromides were performed similarly to the preparation of the mentioned Na–Zn complexes but in solvent mixtures with an optimised chloroform/methanol ratio to ensure sufficient solubility of the alkali metal halide and not suppress separation of the product after the addition of methyl *tert*-butyl ether.[30] Attempted reactions with RbBr and CsBr did not afford any M–Zn complex because these salts separated from the reaction mixture, whereas the analogous reaction of **6a** with $ZnBr_2$ and KBr produced K–Zn complex **9a** (Scheme 4), which adopts the structure of its sodium congener. In contrast, the reaction **6a** with $ZnBr_2$ and LiBr produced a Zn–Li complex $[Zn_2Li_2Br_6(\mathbf{6a})_2(CH_3OH)_4(H_2O)]\cdot CH_3OH$ (**10a**·CH_3OH). In its structure, the phosphinoferrocene ligands coordinate the terminal $ZnBr_3$ units *via* their phosphine groups (similarly to the mentioned Na–Zn and K–Zn complexes) and further bind solvated Li^+ ions *via* the sulfone oxygens to form a discrete pseudodimeric assembly (Scheme 5).[31]

The M–Zn complexes (M = alkali metal cation) disintegrate upon dissolving in donor solvents. This was evidenced by the ^1H and $^{31}P\{^1H\}$ NMR spectra recorded for solutions of crystal-

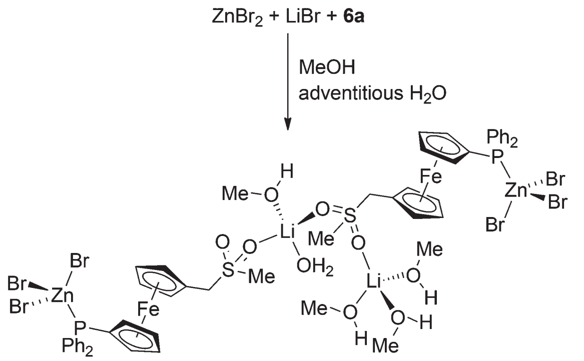

10a

Scheme 5 Preparation of the Li–Zn complex **10a**.

line **8a** in CD_3OD that reveal the exclusive presence of uncoordinated **6a** in solution (δ_P −16.3 ppm) and also by the ESI mass spectra showing only signals due to **6a** and its fragments (see Experimental). The same applies to the elusive **6a**-$ZnBr_2$ complexes (intermediates) as similar features have been observed in the NMR and ESI MS spectra of a residue obtained by evaporation of a 1 : 1 mixture of **6a**-$ZnBr_2$. Hence, the characterisation of the mixed-metal complexes had to be confined to solid-state techniques. Unfortunately, the IR spectra were of little diagnostic value because of their relative complexity (see ESI, Fig. S1†) and only marginal shifts of the diagnostic bands upon coordination (*e.g.*, the bands due to the sulfone moiety as compared to uncoordinated **6a**). Nonetheless, the IR spectra of **8a**, **8b** and **9a** were very similar, suggesting analogous structures for these compounds, and displayed additional broad bands attributable to ν_{OH} vibrations at *ca.* 3470–3490 cm^{-1}, attributable to the "solvating" methanol. Nonetheless, unequivocal structural information was gained from single-crystal X-ray diffraction analysis.

Compounds **8a** and **8b** are essentially isostructural, and the minor differences in the lattice parameters and atomic coordinates are associated with the different sizes of the halide anions. Compound **9a** also has practically the same structure, albeit described by different cell parameters because even a small variation in the cell angles near 90° as in this particular case can result in another reduced triclinic cell setting.[32] The structure of **8a** is depicted in Fig. 7, and the displacement ellipsoid plots for all three compounds are presented in the ESI (Fig. S2–S4†). Pertinent geometric parameters are given in Table 3.

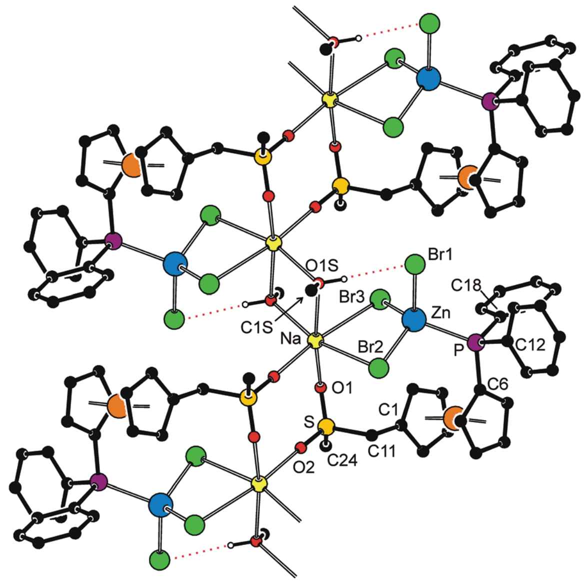

Fig. 7 Section of the infinite coordination chain in the structure of **8a** (for a conventional displacement ellipsoid plot, see the ESI†). For clarity, the CH hydrogens are omitted, and the $CH_3OH\cdots Br$ hydrogen bond is indicated by a red dotted line (O1S⋯Br1 = 3.599(2) Å; the corresponding distance in the structures of **8b** and **9a** are as follows: **8b**, O1S⋯I1 = 3.828(3) Å; **9a**, O1S⋯Br1 = 3.540(2) Å).

Compounds **8a** and **8b** are one-dimensional coordination polymers in which the ZnX_3(**6a**-κ*P*) units coordinate the Na(I) ions *via* two halide ions (bridging X2 and X3) and the sulfone oxygen O1. The coordination sphere of the Na(I) ion is completed by the sulfone O2 located in an adjacent ZnX_3(**6a**-κ*P*) moiety, related by crystallographic inversion, and also by a methanol molecule and its inversion-related counterpart. The solvating methanol further stabilises the structure through a hydrogen bond with the Zn-bound halide (O1S–H1O⋯X1, see Fig. 7).

The Zn(II) ions in the structures of **8a** and **8b** have the usual, albeit distorted, tetrahedral donor environment (donor set: PX_3), where two Zn–X distances are somewhat shorter than the remaining one (Zn–X1/2 < Zn–X3). The associated interligand angles increase in the following order: X1–Zn–X3 < X2–Zn–P ≈ X2–Zn–X3 < X1–Zn–P ≈ X1–Zn–X2 < X3–Zn–P (*cf.* the ranges of 102.64(2)–114.50(2)° and 101.61(1)–114.68(3)° for **8a** and **8b**, respectively). In contrast, the sodium cation, as the second metal centre in the structures, has an unsymmetric octahedral coordination (donor set: *cis*-X_2O_4), wherein the extreme Na-donor distances differ by *ca.* 0.8 and 1.1 Å and the interligand angles (*cis*-only) span the ranges of 78.25(7)–101.12(8)° and 77.1(1)–104.7(1)° for **8a** and **8b**, respectively. In both cases, the Na atoms appear displaced from the geometrical centre of the octahedron towards O1S^{ii} and O2^{i} in heavily twisted pseudoequatorial planes {Na, X2, X3, O1S^{ii}, O2^{i}}. The observed angular distortions of the coordination spheres around both the Zn(II) and Na(I) ions appear to result from an interplay between the unlike metal–donor distances, steric requirements of the individual donors, constraints imposed by the doubly bridged fragments (Zn(μ-Br)$_2$Na and Na-(μ-CH_3OH)$_2$Na), and the hydrogen-bond interactions.

Table 3 Selected distances and angles for **8a**, **8b**, and **9a** (in Å and °)[a]

Parameter	**8a** (M/X = Na/Br)	**8b** (M/X = Na/I)	**9a** (M/X = K/Br)
Zn–P	2.4304(8)	2.445(1)	2.4310(6)
Zn–X1	2.3965(4)	2.6030(4)	2.4065(4)
Zn–X2	2.3980(4)	2.5956(4)	2.4049(4)
Zn–X3	2.4517(4)	2.6610(4)	2.4440(3)
M–X2	3.089(1)	3.362(2)	3.3218(6)
M–X3	3.010(1)	3.244(2)	3.2865(6)
M–O1	2.512(2)	2.485(3)	2.725(2)
M–O2$^{i/iii}$	2.260(2)^{i}	2.264(3)^{i}	2.576(2)^{iii}
M–O1S	2.616(2)	2.686(3)	2.829(2)
M–O1S$^{ii/iv}$	2.387(2)^{ii}	2.399(3)^{ii}	2.730(2)^{iv}
Fe–C	2.024(3)–2.051(3)	2.034(3)–2.043(4)	2.027(2)–2.056(2)
Tilt	4.1(2)	4.1(2)	5.1(1)
C1–Cg1–Cg2–C6	−85.6(2)	−84.7(2)	−85.4(1)
S–O1	1.446(2)	1.450(3)	1.444(2)
S–O2	1.439(2)	1.437(3)	1.442(2)

[a] For definitions, see the footnote to Table 2. Symmetry codes: (i) 2 − *x*, −*y*, −*z*, (ii) 1 − *x*, −*y*, −*z*, (iii) 1 − *x*, 1 − *y*, −*z*; (iv) −*x*, 1 − *y*, −*z*.

As indicated above, the structure of **9a** is very similar to its Na congener **8a**, with the observed differences reflecting the larger size of the alkali metal cation present in the structure. The geometry of the $PZnBr_3$ moiety remains virtually unchanged upon going from **8a** to **9a**; the interligand angles span the range 102.97(1)–113.11(2)° and follow the trend described for **8a** though not with the same differences between the individual values. Although the overall coordination environment of the K^+ ion also remains seemingly the same (*cis*-interligand angles: 74.02(1)–107.97(5)°), the coordination sphere is expanded because of the longer potassium-donor bonds (by approximately 0.21–0.34 Å in the respective pairs).

The structure of **10a**·CH_3OH (Fig. 8, parameters in Table 4) reveals that the replacement of Na^+ with the Li^+ ion, which is smaller and prefers a tetrahedral coordination environment, results in an opening of the polymeric structure and incorporation of solvent molecules as additional donors into the structure. One of the Li^+ cations (Li1) is coordinated by a sulfonate oxygen (O2) and three methanol molecules (O*n*S, *n* = 1–3) constituting a tetrahedral donor set. The other Li^+ cation (Li2) has a similar coordination, binding two sulfonate oxygens (from different molecules of **6a**), methanol (O4S) and water molecule (O1W). It is noteworthy that the asymmetric environment of the sulfur atoms renders the structure chiral.

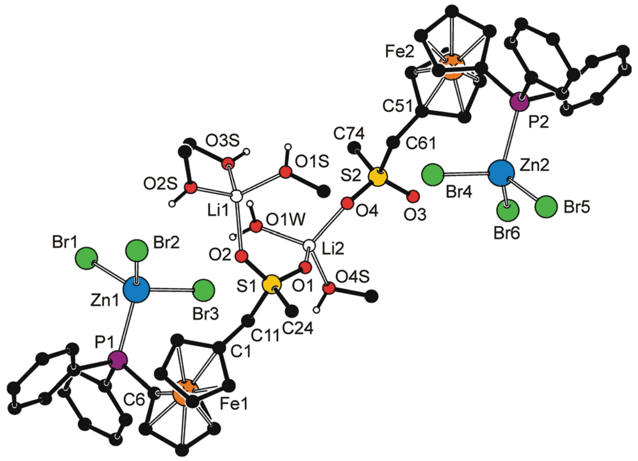

Fig. 8 Perspective drawing of the structure of **10a**·CH_3OH. The molecule of solvating methanol and CH hydrogens are omitted for clarity. For a displacement ellipsoid plot, see the ESI (Fig. S5†).

Table 4 Selected distances and angles for **10a**·CH_3OH (in Å and °)[a]

Zn1–P1	2.437(1)	Zn2–P2	2.442(1)
Zn1–Br1	2.4174(8)	Zn2–Br4	2.3763(8)
Zn1–Br2	2.4016(8)	Zn2–Br5	2.4056(8)
Zn1–Br3	2.4034(8)	Zn2–Br6	2.4362(8)
Li1–O2	1.98(1)	Li2–O1	1.917(8)
Li1–O1S	1.94(1)	Li2–O4	1.907(9)
Li1–O2S	1.911(9)	Li2–O4S	1.916(9)
Li1–O3S	1.962(9)	Li2–O1W	1.92(1)
O–Li1–O	100.9(4)–123.8(5)	O–Li2–O	99.1(4)–114.4(4)
Fe1–C	2.028(6)–2.052(5)	Fe2–C	2.020(6)–2.053(6)
Tilt	5.2(3)	Tilt	5.5(3)
C1–Cg1–Cg2–C6	−81.6(4)	C1–Cg1–Cg2–C6	82.2(4)
S1–O1	1.433(3)	S2–O3	1.443(4)
S1–O2	1.451(4)	S2–O4	1.454(3)

[a] For definitions, see the footnote to Table 2.

On the other hand, the halide anion is transferred to the zinc(II) centre, which thus gains a distorted tetrahedral PBr_3 coordination as observed for the Na/K–Zn complexes discussed above. Both $ZnBr_3$ units in the structure of **10a** assume a sterically loose staggered orientation with respect to their bonding PC_3 moieties and do not exert any pronounced angular distortion (*cf.* the interligand angles ranging 105.64(4)–114.28(4)° for Zn1 and 104.54(3)–112.79(4)° for Zn2).

Conclusion

Alkylation of phosphinoamine **1** with 1,3-propanesultone proceeds selectively under alkylation of the hard nitrogen group to afford the quaternary ammonium salt **2**. Betaine **2**, possessing an intact phosphine substituent, is an attractive functionalised starting material for ferrocenylmethylation reactions with nucleophiles, which was demonstrated in this paper by model reactions leading to **3** and **4**, and by the synthesis of the phosphinosulfones **6** representing new entries among hybrid[33] phosphinoferrocene donors possessing flexible methylene spacers.[6–11] Compound **6a**, chosen as a representative phosphinosulfone donor, was shown to form unprecedented[34] alkali metal–Zn coordination polymers of the general formula $[ZnMX_3(\mathbf{6a})(CH_3OH)]_n$ (M/X = Na/Br, Na/I, and K/Br), in which the ferrocene-based ligand coordinates the softer Zn(II) ion *via* its phosphine substituent and the alkali metal cation through the sulfone oxygen atoms, while the methanol molecules complete octahedral coordination around the alkali metal ions. These compounds are zwitterions combining negatively charged $ZnBr_3$ units with cationic centres represented by the alkali metal cations in their structures. In the case of $ZnBr_2$–LiBr, the analogous reaction with **6a** provides $[Br_3Zn(\mathbf{6a})Li_2(CH_3OH)_4(H_2O)(\mathbf{6a})ZnBr_3]$ (methanol solvate), a pseudodimeric complex comprising two chemically different, tetrahedral Li^+ centres coordinated by the sulfonate oxygens, solvating methanol and a water molecule, and the phosphine-coordinated $ZnBr_3$ units.

Experimental

Materials and methods

All reactions were performed under an argon atmosphere by standard Schlenk techniques. Amine **1** was prepared as reported previously.[10] Benzene and chloroform were dried by standing over sodium metal and CaH_2, respectively, and distilled under argon. Dimethyl sulfoxide was distilled under vacuum. Methanol was dried with an in-house PureSolv MD5 solvent-drying system (Innovative Technology, USA). A solution of sodium methoxide was prepared by dissolving the appropriate amount of sodium metal in anhydrous methanol. Other chemicals and solvents were obtained from commercial suppliers (Sigma-Aldrich or Lachner, Czech Republic) and were used without any additional purification.

NMR spectra were recorded at 25 °C on a Varian Unity INOVA spectrometer operating at 399.95 MHz for ^{1}H, 100.58 MHz for ^{13}C, and 161.92 MHz for ^{31}P. The chemical shifts (δ in ppm) are given relative to internal tetramethylsilane (^{1}H and ^{13}C) or to external 85% aqueous H_3PO_4 (^{31}P). IR spectra were obtained on a Nicolet Magna 6700 FTIR spectrometer in the range of 400–4000 cm^{-1}. Electrospray ionisation mass spectra (ESI MS) were acquired with a Bruker Esquire 3000 spectrometer using samples dissolved in HPLC-grade methanol.

Syntheses

Synthesis of betaine 2. A solution of propane-1,3-sultone (1.221 g, 10 mmol) in dry benzene (30 mL) was slowly introduced into a solution of amine **1** in the same solvent (4.272 g, 10 mmol in 20 mL). The resultant mixture was stirred at room temperature overnight (15 h), during which time a fine yellow precipitate deposited. The reaction mixture was diluted with methanol (50 mL) and carefully evaporated. The residue was purified by column chromatography over silica gel, eluting first with dichloromethane–methanol (5 : 1) to remove the less polar impurities. The polarity of the eluent was then increased (dichloromethane–methanol 3 : 1) to elute a salt containing the protonated amine **1** as the cation, very likely hydrochloride [**1**H]Cl.[35] Finally, the eluent was changed to dichloromethane–methanol 1 : 1, which removed the major orange band of the desired product. Following evaporation and drying under vacuum over sodium hydroxide, betaine **2** was isolated as an air-stable orange solid (4.476 g, 81%). An analytical sample, in the form of the defined solvate **2**·CH_3OH, was obtained upon crystallisation from methanolic solution layered with tetrahydrofuran and diethyl ether.

Analytical data for betaine 2. ^{1}H NMR (DMSO-d$_6$): δ 1.99 (m, 2 H, $NCH_2CH_2CH_2SO_3$), 2.45 (t, $^3J_{HH}$ = 7.1 Hz, 2 H, $NCH_2CH_2CH_2SO_3$), 2.78 (s, 6 H, $N(CH_3)_2$), 3.21 (m, 2 H, $NCH_2CH_2CH_2SO_3$), 4.04 (s, 2 H, $C_5H_4CH_2$), 4.16 (vq, J' = 1.9 Hz, 2 H, PC_5H_4), 4.22 (vt, J' = 1.9 Hz, 2 H, $CH_2C_5H_4$), 4.44 (vt, J' = 1.9 Hz, 2 H, $CH_2C_5H_4$), 4.53 (vt, J' = 1.9 Hz, 2 H, PC_5H_4), 7.30–7.43 (m, 10 H, PPh_2). ^{31}P{^{1}H} NMR (DMSO-d$_6$): δ −18.1 (s). ^{13}C{^{1}H} NMR (DMSO-d$_6$): δ 18.89 (s, $NCH_2CH_2CH_2SO_3$), 47.63 (s, $NCH_2CH_2CH_2SO_3$), 48.86 (s, NMe_2), 62.03 (s, $NCH_2CH_2CH_2SO_3$), 63.04 (s, $C_5H_4CH_2$), 71.04 (s, CH of $CH_2C_5H_4$), 71.95 (d, $^3J_{PC}$ = 4 Hz, β-CH of PC_5H_4), 72.86 (s, CH of $CH_2C_5H_4$), 73.35 (s, C_{ipso} of $CH_2C_5H_4$), 73.48 (d, $^2J_{PC}$ = 15 Hz, α-CH of PC_5H_4), 76.68 (d, $^1J_{PC}$ = 9 Hz, C_{ipso} of PC_5H_4), 128.33 (d, $^3J_{PC}$ = 7 Hz, CH_{meta} of PPh_2), 128.71 (s, CH_{para} of PPh_2), 133.00 (d, $^2J_{PC}$ = 20 Hz, CH_{ortho} of PPh_2), 138.33 (d, $^1J_{PC}$ = 10 Hz, C_{ipso} of PPh_2). IR (Nujol): ν_{max} 3420 br m, 2723 vw, 2669 vw, 1656 m, 1649 m, 1643 m, 1584 w, 1568 vw, 1308 m, 1189 br vs ($\nu_a(SO_3)$), 1094 m, 1069 m, 1037 vs ($\nu_s(SO_3)$), 998 m, 920 w, 889 m, 842 m, 820 m, 743 s, 727 m, 697 s, 634 w, 619 w, 602 m, 570 w, 548 w, 523 m, 501 m, 489 m, 456 m, 408 vw cm^{-1}. MS (ESI+): m/z 383 ($[Ph_2PfcCH_2]^+$), 550 ($[Ph_2PfcCH_2NMe_2(CH_2)_3SO_3 + H]^+$), 572 ($[Ph_2PfcCH_2NMe_2(CH_2)_3SO_3 + Na]^+$), 588 ($[Ph_2PfcCH_2NMe_2(CH_2)_3SO_3 + K]^+$). Anal. calc. for $C_{28}H_{32}FeNO_3PS \cdot MeOH$ (581.5): C 59.90, H 6.24, N 2.41%. Found: C 59.66, H 5.84, N 2.39%.

Preparation of alcohol 3. Degassed aqueous NaOH (25 mL of 2 M solution) was slowly added to a solution of betaine **2** (1.099 g, 2.0 mmol) in dimethyl sulfoxide (25 mL) heated in an oil bath maintained at 130 °C. The refluxing reaction mixture was stirred for 1 h, during which time it darkened and deposited as a brown precipitate. The mixture was cooled to room temperature and diluted with water (50 mL), and the resulting mixture was extracted with dichloromethane (3 × 50 mL). The combined organic layers were washed with water (2 × 200 mL), dried over magnesium sulfate, and evaporated. The residue was purified by column chromatography on a silica-gel column. Elution with diethyl ether–hexane (1 : 10) resulted in a yellow band that contained compound **5**, which was isolated in a 6% yield (44 mg) after evaporation. Subsequent elution with diethyl ether–hexane 2 : 1 led to the development of a major orange band due to alcohol **3**, which was isolated as slowly crystallising orange oil upon evaporation under vacuum. Yield of **3**: 511 mg (64%). The compound was identified by NMR spectroscopy.[12a]

Analytical data for 5. ^{1}H NMR ($CDCl_3$): δ 1.81 (s, 3 H, CH_3), 3.92 (vt, J' = 1.8 Hz, 2 H), 3.99 (vt, J' = 1.8 Hz, 2 H), 4.00 (vt, J' = 1.9 Hz, 2 H) and 4.29 (vt, J' = 1.9 Hz, 2 H) (4 × CH of C_5H_4), 7.28–7.40 (m, 10 H, $P(C_6H_5)_2$) ppm. ^{31}P{^{1}H} NMR ($CDCl_3$): δ −16.0 (s) ppm. ^{13}C{^{1}H} NMR ($CDCl_3$): δ 14.40 (s, CH_3), 68.41 (s, CH of MeC_5H_4), 70.23 (s, CH of MeC_5H_4), 71.66 (d, $^3J_{PC}$ = 4 Hz, CH of PC_5H_4), 73.45 (d, $^2J_{PC}$ = 15 Hz, CH of MeC_5H_4), 84.67 (s, C_{ipso} of MeC_5H_4), 128.07 (d, $^3J_{PC}$ = 7 Hz, CH_{meta} in PPh_2), 128.40 (s, CH_{para} in PPh_2), 133.51 (d, $^2J_{PC}$ = 20 Hz, CH_{ortho} in PPh_2), 139.22 (d, $^1J_{PC}$ = 10 Hz, C_{ipso} in PPh_2) ppm. The signal of C_{ipso} of PC_5H_4 is probably obscured by the solvent resonance. MS (ESI+): m/z 200 ($[FcCH_3]^{+\bullet}$), 384 ($[Ph_2PfcCH_3]^{+\bullet}$). Anal. calc. for $C_{23}H_{21}FeP$ (400.2): C 71.89, H 5.51%. Found: C 71.72, H 5.41%.

Preparation of ether 4. Betaine **2** (1.101 g, 2.0 mmol) was dissolved in dimethyl sulfoxide (25 mL) at 100 °C, and the solution was treated with 2 M MeONa in methanol (25 mL). The resulting mixture was heated under reflux for 2 h and cooled to room temperature. Then, it was diluted with water (50 mL) and extracted with dichloromethane (3 × 50 mL). The organic extracts were washed with water (2 × 200 mL), dried over magnesium sulfate, and evaporated. The crude product was purified by chromatography over a silica-gel column using diethyl ether–hexane 1 : 1 as the eluent. The major band due to the product was collected and evaporated under vacuum to yield ether **4** as a yellow-orange solid. Yield: 388 mg (47%). The NMR spectra of the product were identical with those reported in the literature.[9]

Preparation of 6a. A solution of sodium methanesulfinate (0.534 g, 5.0 mmol) in degassed water (25 mL) was added to a solution of betaine **2** (1.097 g, 2.0 mmol) in dimethylsulfoxide (25 mL) kept in an oil bath preheated to 130 °C. The resulting solution was heated under reflux for 2 h, whereupon it turned brown, and a yellow-brown precipitate separated. The reaction mixture was cooled to room temperature, diluted with water (50 mL), and extracted with dichloromethane (3 × 50 mL). The combined organic layers were diluted with dichloromethane (50 mL), washed with water (2 × 200 mL), dried over anhydrous magnesium sulfate, and evaporated under reduced pressure. The residue was purified by chromatography over a silica-gel column, first using dichloromethane–methanol 50 : 1 to elute the main orange band of **6a** and a small tailing band containing alcohol **3**. The mobile phase was then changed to dichloromethane–methanol 20 : 1, which led to the development of an additional broad yellow band containing the side product **7**. The complete separation of **3** and **6a** was achieved through additional chromatography over silica gel using ethyl acetate–hexane (1 : 2) as the eluent (note: the alcohol elutes first under such conditions) or, alternatively, *via* crystallisation from ethyl acetate/hexane. Yields: **6a** – yellow solid (272 mg, 29%); **3** – orange, slowly crystallising oil (14 mg, 2%); and **7** – rusty brown oil (74 mg, 12%).

Analytical data for ***6a***. ^{1}H NMR ($CDCl_3$): δ 2.62 (s, 3 H, SO_2Me), 3.59 (s, 2 H, $C_5H_4CH_2$), 4.10 (vq, J' = 1.8 Hz, 2 H), 4.19 (vt, J' = 1.9 Hz, 2 H), 4.26 (vt, J' = 1.9 Hz, 2 H) and 4.40 (vt, J' = 1.8 Hz, 2 H) (4 × CH in fc); 7.31–7.41 (m, 10 H, PPh_2). $^{31}P\{^1H\}$ NMR ($CDCl_3$): δ −17.0 (s). $^{13}C\{^1H\}$ NMR ($CDCl_3$): δ 38.43 (SO_2Me), 56.65 (s, $C_5H_4CH_2$), 70.59 (s, CH of $CH_2C_5H_4$), 71.07 (s, CH of $CH_2C_5H_4$), 71.73 (d, $^3J_{PC}$ = 4 Hz, β-CH of PC_5H_4), 74.03 (d, $^2J_{PC}$ = 15 Hz, α-CH of PC_5H_4), 74.88 (s, C_{ipso} of $CH_2C_5H_4$), 128.31 (d, $^3J_{PC}$ = 7 Hz, CH_{meta} of PPh_2), 128.80 (s, CH_{para} of PPh_2), 133.50 (d, $^2J_{PC}$ = 20 Hz, CH_{ortho} of PPh_2), 138.67 (d, $^1J_{PC}$ = 10 Hz, C_{ipso} of PPh_2). The resonance of ferrocene *C*–P was not found. IR (Nujol): ν_{max} 3015 m, 2725 vw, 2282 vw, 1583 w, 1567 vw, 1435 s, 1419 w, 1412 w, 1397 w, 1322 m, 1304 vs ($\nu_{as}(SO_2)$), 1286 m, 1242 w, 1228 w, 1192 w, 1161 m, 1139 vs ($\nu_s(SO_2)$), 1122 m, 1099 m, 1084 vw, 1069 w, 1058 vw, 1038 m, 1023 m, 998 w, 963 s, 928 m, 903 vw, 843 m, 835 m, 788 s, 750 s, 742 vs, 704 s, 697 vs, 630 w, 618 vw, 603 w, 569 vw, 529 m, 510 m, 486 s, 479 vs, 455 s, 441 m, 406 vw cm^{-1}. MS (ESI+): *m/z* 383 ($[Ph_2PfcCH_2]^+$), 463 ($[\mathbf{6a} + H]^+$), 485 ($[\mathbf{6a} + Na]^+$), 501 ($[\mathbf{6a} + K]^+$). Anal. calc. for $C_{24}H_{23}FeO_2PS$ (462.3): C 62.35, H 5.01%. Found: C 62.59, H 4.82%.

Analytical data for ***7***. ^{1}H NMR ($CDCl_3$): δ 3.59 (d, $^2J_{PH}$ = 12.7 Hz, 2 H, PCH_2), 3.83 (d of vt, *J* = 1.9, 0.8 Hz, 2 H), 3.94 (vt, J' = 1.9 Hz, 2 H), 4.02 (vt, J' = 1.9 Hz, 2 H) and 4.33 (vt, J' = 1.9 Hz, 2 H) (4 × CH in fc); 6.12 (m, 2 H, α-CH of $P{=}C_5H_4$), 6.40 (m, 2 H, β-CH of $P{=}C_5H_4$), 7.25–7.35 (m, 10 H, $fcPPh_2$), 7.41–7.47 (m, 8 H, CH_{ortho} and CH_{meta} of CH_2PPh_2), 7.55–7.61 (m, 2 H, CH_{para} of CH_2PPh_2). $^{31}P\{^1H\}$ NMR ($CDCl_3$): δ −16.9 (s, $fcPPh_2$), 10.1 (s, $CH_2P{=}C_5H_4$). $^{13}C\{^1H\}$ NMR ($CDCl_3$): δ 30.01 (dd, $^1J_{PC}$ = 53 Hz, J_{PC} = 1 Hz, PCH_2), 69.50 (s, CH of fc), 71.49 (s, CH of fc), 71.77 (d, $^3J_{PC}$ = 4 Hz, CH of fc), 73.89 (d, $^2J_{PC}$ = 15 Hz, CH of fc), 77.42 (d, $^2J_{PC}$ = 2 Hz, C_{ipso} of fc), 78.21 (d, $^1J_{PC}$ = 110 Hz, C_{ipso} of $P{=}C_5H_4$), 113.92 (d, $^2J_{PC}$ = 18 Hz, α-CH of $P{=}C_5H_4$), 115.83 (d, $^3J_{PC}$ = 15 Hz, β-CH of $P{=}C_5H_4$), 125.49 (d, $^1J_{PC}$ = 86 Hz, C_{ipso} of CH_2PPh_2), 128.19 (d, $^3J_{PC}$ = 7 Hz, CH_{meta} of CH_2PPh_2), 128.59 (d, $^2J_{PC}$ = 12 Hz, CH_{ortho} of $fcPPh_2$), 128.63 (s, CH_{para} of $fcPPh_2$), 132.54 (d, $^4J_{PC}$ = 3 Hz, CH_{para} of CH_2PPh_2), 133.37 (s, CH_{meta} of $fcPPh_2$), 133.52 (d, $^2J_{PC}$ = 10 Hz, CH_{ortho} of CH_2PPh_2), 138.85 (d, $^1J_{PC}$ = 10 Hz, C_{ipso} of $fcPPh_2$). MS (ESI+): *m/z* 383 ($[Ph_2PfcCH_2]^+$), 633 ($[\mathbf{7} + H]^+$). HRMS (APCI+) calc. for $C_{40}H_{35}FeP_2$ ($[M + H]^+$): 633.1558, found: 633.1561. Anal. calc. for $C_{40}H_{34}FeP_2\cdot 1/8CHCl_3$ (647.4): C 74.44, H 5.31%. Found: C 74.30, H 5.38%.

Preparation of 6b. Betaine **2** (2.0 mmol) was dissolved in dimethylsulfoxide (25 mL), and the reaction flask was transferred to an oil-bath preheated to 130 °C. After stirring for several minutes at this temperature, an aqueous solution of the corresponding sulfinate (5.0 mmol in 25 mL of degassed water) was added, and the resultant mixture was heated under reflux for 2 h (an orange precipitate separated). The reaction mixture was cooled to room temperature, diluted with water (50 mL), and extracted with dichloromethane (3 × 50 mL). The combined organic layers were diluted with dichloromethane (50 mL), washed with water (2 × 200 mL), dried over magnesium sulfate, and evaporated under vacuum. The products were isolated by column chromatography over silica gel. Initial elution with dichloromethane–methanol 50 : 1 produced a major orange band due to sulfone **6**, followed by a minor band of alcohol **3**. Subsequent elution with dichloromethane–methanol 20 : 1 led to the development of a broad yellow band containing crude **7**. Compound **3** was further purified as described above (see the preparation of **3**). Particular details are as follows.

The reaction of **2** (1.099 g, 2.0 mmol) with sodium phenylsulfinate (0.838 g, 5.0 mmol) as described above yielded **6b** (yellow solid; 524 mg, 50%), **3** (14 mg, 2%), and **7** (61 mg, 10%). Starting with **2** (1.095 g, 2.0 mmol) and sodium 4-toluenesulfinate (0.937 g, 5.0 mmol), an analogous procedure produced **6c** (yellow solid; 570 mg, 53%), **3** (25 mg, 3%), and **7** (98 mg, 16%).

Analytical data for ***6b***. ^{1}H NMR ($CDCl_3$): δ 3.68 (s, 2 H, $C_5H_4CH_2$), 3.94 (vt, J' = 1.9 Hz, 2 H), 4.02 (vq, J' = 1.8 Hz, 2 H), 4.05 (vt, J' = 1.9 Hz, 2 H) and 4.32 (vt, J' = 1.8 Hz, 2 H) (4 × CH of fc), 7.28–7.35 (m, 10 H, PPh_2), 7.42–7.47 (m, 2 H, SO_2Ph), 7.57–7.62 (m, 3 H, SO_2Ph). $^{31}P\{^1H\}$ NMR ($CDCl_3$): δ −16.9 (s). $^{13}C\{^1H\}$ NMR ($CDCl_3$): δ 58.23 (s, $C_5H_4CH_2$), 70.16 (s, CH of $CH_2C_5H_4$), 71.30 (s, CH of $CH_2C_5H_4$), 71.52 (d, $^3J_{PC}$ = 4 Hz, β-CH of PC_5H_4), 73.81 (d, $^2J_{PC}$ = 15 Hz, α-CH of PC_5H_4), 74.68 (s, C_{ipso} of $CH_2C_5H_4$), 76.79 (d, $^1J_{PC}$ = 7 Hz, C_{ipso} of PC_5H_4), 128.24 (d, $^3J_{PC}$ = 7 Hz, CH_{meta} of PPh_2), 128.69 (s, CH_{ortho} and CH_{meta} of SO_2Ph + CH_{para} of PPh_2), 133.44 (d, $^2J_{PC}$ = 20 Hz, CH_{ortho} of PPh_2), 133.51 (s, CH_{para} of SO_2Ph), 137.84 (s, C_{ipso} of SO_2Ph), 138.73 (d, $^1J_{PC}$ = 10 Hz, C_{ipso} of PPh_2). IR (Nujol): ν_{max} 2723 vw, 2667 vw, 1583 vw, 1568 vw, 1400 w, 1311 s, 1304 vs ($\nu_{as}(SO_2)$), 1288 m, 1263 w, 1240 vw, 1223 vw, 1149 vs, ($\nu_s(SO_2)$), 1110 w, 1086 m, 1068 w, 1058 vw, 1036 w, 1029 m, 999 vw, 974 vw, 927 w, 888 vw, 880 vw, 871 vw, 834 m, 761 m, 749 s, 708 m, 700 m, 686 m, 633 w, 614 w, 571 s, 549 vw, 531 w, 503 s, 490 s, 458 m, 432 vw, cm^{-1}. MS (ESI+): *m/z* 383 ($[Ph_2PfcCH_2]^+$), 525 ($[\mathbf{6b} + H]^+$), 547 ($[\mathbf{6b} + Na]^+$), 563 ($[\mathbf{6b} + K]^+$). Anal. calc. for

$C_{29}H_{25}FeO_2PS$ (524.4): C 66.42, H 4.81%. Found: C 66.20, H 4.80%.

Analytical data for ***6c****.* ^{1}H NMR ($CDCl_3$): δ 2.43 (s, 3 H, $C_6H_4CH_3$), 3.67 (s, 2 H, $C_5H_4CH_2$), 3.95 (vt, J' = 1.9 Hz, 2 H), 4.02 (vq, J' = 1.8 Hz, 2 H), 4.06 (vt, J' = 1.9 Hz, 2 H) and 4.32 (vt, J' = 1.8 Hz, 2 H) (4 × CH of fc), 7.23–7.26 (m, 2 H, C_6H_4), 7.29–7.35 (m, 10 H, PPh_2), 7.46–7.50 (m, 2 H, C_6H_4). ^{31}P{^{1}H} NMR ($CDCl_3$): δ −16.9 (s). ^{13}C{^{1}H} NMR ($CDCl_3$): δ 21.64 (s, $C_6H_4CH_3$), 58.28 (s, $C_5H_4CH_2$), 70.14 (s, CH of $CH_2C_5H_4$), 71.33 (s, CH of $CH_2C_5H_4$), 71.50 (d, $^3J_{PC}$ = 4 Hz, β-CH of PC_5H_4), 73.78 (d, $^2J_{PC}$ = 14 Hz, α-CH of PC_5H_4), 74.86 (s, C_{ipso} of $CH_2C_5H_4$), 76.77 (d, $^1J_{PC}$ = 7 Hz, C_{ipso} of PC_5H_4), 128.24 (d, $^3J_{PC}$ = 7 Hz, CH_{meta} of PPh_2), 128.69 (s), 128.71 (s) and 129.32 (s) (2 × CH of C_6H_4 + CH_{para} of PPh_2), 133.45 (d, $^2J_{PC}$ = 20 Hz, CH_{ortho} of PPh_2), 134.96 (s, CSO_2 of C_6H_4), 138.75 (d, $^1J_{PC}$ = 10 Hz, C_{ipso} of PPh_2), 144.43 (s, CCH_3 of C_6H_4). IR (Nujol): ν_{max} 2726 vw, 2669 vw, 1594 w, 1436 m, 1403 w, 1319 vs ($\nu_{as}(SO_2)$), 1301 m, 1289 m, 1259 m, 1221 m, 1194 vw, 1183 vw, 1148 vs ($\nu_s(SO_2)$), 1117 w, 1106 m, 1086 s, 1070 w, 1053 vw, 1047 vw, 1038 w, 1027 m, 998 vw, 926 w, 888 w, 875 m, 868 w, 848 vw, 837 m, 824 m, 813 m, 799 w, 750 s, 698 s, 633 m, 611 w, 552 m, 513 s, 497 s, 485 m, 469 w, 453 m, 440 vw, 431 vw cm^{-1}. MS (ESI+): *m*/*z* 383 ([Ph_2PfcCH_2]$^+$), 539 ([**6c** + H]$^+$), 561 ([**6c** + Na]$^+$). Anal. calc. for $C_{30}H_{27}FeO_2PS$ (538.4): C 66.92, H 5.06%. Found: 66.62, H 5.00%.

Preparation of 8a. A methanolic solution of sodium bromide (10.3 mg, 0.10 mmol in 0.6 mL) was added to solid $ZnBr_2$ (22.5 mg, 0.10 mmol), followed by a solution of sulfone **6a** in chloroform (46.2 mg, 0.10 mmol in 0.6 mL). The resulting mixture was stirred for 30 min, filtered through a PTFE syringe filter (0.45 µm pore size), and diluted with additional methanol (0.3 mL) as the top layer. The filtrate was layered with methyl *tert*-butyl ether to a total volume of 10 mL, and the mixture was set aside for crystallisation. The orange crystals, which separated over several days, were filtered off, washed three times with methyl *tert*-butyl ether, and dried under vacuum. Yield of **8a**: 64.6 mg (79%).

IR (Nujol): ν_{max} 3495 br m, 3090 m, 2724 vw, 2670 vw, 1618 w, 1433 m, 1410 w, 1354 w, 1317 m, 1303 vs, 1269 m, 1248 vw, 1228 w, 1193 vw, 1169 m, 1145 s, 1119 s, 1096 w, 1065 vw, 1052 vw, 1043 vw, 1030 m, 1022 m, 1006 m, 971 m, 953 w, 931 w, 904 vw, 890 m, 857 w, 847 w, 828 w, 792 w, 751 s, 705 w, 694 m, 629 w, 610 w, 571 vw, 543 w, 518 m, 490 s, 457 m, 434 vw cm^{-1}. MS (ESI+): *m*/*z* 383 ([Ph_2PfcCH_2]$^+$), 463 ([**6a** + H]$^+$), 485 ([**6a** + Na]$^+$), 501 ([**6a** + K]$^+$). Anal. calc. for $C_{25}H_{27}Br_3FeNaO_3PSZn$ (822.4): C 36.51, H 3.31%. Found: C 36.64, H 3.37%.

Preparation of 8b. Compound **8b** was prepared similarly to **8a** but using different amounts of solvents. Thus, a solution of NaI (15.0 mg, 0.10 mmol) in methanol (0.3 mL) and a chloroform solution of **6a** (46.2 mg, 0.10 mmol in 0.6 mL) were successively added to ZnI_2 (31.9 mg, 0.10 mmol). The resultant mixture was stirred for 30 min, filtered (PTFE syringe filter as above), and layered with methanol (0.1 mL) and methyl *tert*-butyl ether (up to 10 mL total volume). Crystallisation by diffusion over several days produced an orange crystalline solid, which was filtered off, washed three times with methyl *tert*-butyl ether, and dried under vacuum. Yield: 78.4 mg (81%).

IR (Nujol): ν_{max} 3490 br m, 3099 w, 3091 m, 2724 vw, 2670 vw, 1618 w, 1435 m, 1407 w, 1314 m, 1299 vs, 1267 m, 1227 w, 1192 w, 1166 m, 1143 s, 1118 m, 1107 m, 1095 m, 1090 m, 1062 w, 1052 vw, 1042 w, 1030 m, 1021 m, 1000 m, 970 m, 953 w, 931 w, 887 m, 879 w, 854 w, 847 w, 834 w, 828 w, 790 w, 774 vw, 749 s, 704 w, 692 m, 627 w, 608 w, 570 w, 541 w, 517 m, 499 m, 490 s, 457 m, 432 vw cm^{-1}. MS (ESI+): *m*/*z* 383 ([Ph_2PfcCH_2]$^+$), 463 ([**6a** + H]$^+$), 485 ([**6a** + Na]$^+$), 501 ([**6a** + K]$^+$). Anal. calc. for $C_{25}H_{27}FeI_3NaO_3PSZn$ (963.4): C 31.17, H 2.82%. Found: C 31.44, H 2.86%.

Synthesis of 9a. Using an analogous procedure, a solution of KBr (11.9 mg, 0.10 mmol) in methanol (1.6 mL) was added to solid $ZnBr_2$ (22.6 mg, 0.10 mmol) followed by a chloroform solution of **6a** (46.3 mg, 0.10 mmol in 0.4 mL). The resulting mixture was stirred for 30 min and filtered through a PTFE syringe filter. The filtrate was diluted with methanol (0.5 mL) and layered with methyl *tert*-butyl ether (up to a total volume of 10 mL). Crystallisation by liquid-phase diffusion afforded **9a** as orange crystals, which were isolated as above. Yield: 36.7 mg (44%). Note: some unreacted KBr typically remains on the walls of the reaction vessel as a fine white precipitate.

IR (Nujol): ν_{max} 3475 br m, 3089 m, 1619 w, 1433 m, 1407 w, 1318 m, 1293 s, 1267 m, 1228 w, 1193 w, 1167 m, 1146 s, 1118 m, 1107 m, 1091 m, 1064 w, 1052 vw, 1043 w, 1030 m, 1021 m, 1013 s, 971 m, 960 m, 931 w, 905 w, 890 m, 881 w, 857 w, 846 w, 826 w, 790 w, 748 s, 704 w, 692 s, 627 w, 610 w, 543 w, 517 m, 499 s, 489 s, 459 s, 409 w cm^{-1}. Anal. calc. for $C_{25}H_{27}Br_3FeKO_3PSZn$ (838.5): C 35.81, H 3.25%. Found: C 35.61, H 3.29%.

Preparation of 10a. $ZnBr_2$ (22.6 mg, 0.10 mmol) and LiBr (8.7 mg, 0.10 mmol) were dissolved in methanol (0.10 mL). A chloroform solution of ligand **6a** (46.3 mg, 0.10 mmol in 0.4 mL) was added and the resultant mixture was stirred for 30 min. Filtration, addition of methanol (0.1 mL), addition of methyl *tert*-butyl ether (up to 10 mL total volume) and crystallisation as described above gave **10a** as an orange crystalline solid, which was isolated by suction, washed with methyl *tert*-butyl ether, and dried under vacuum. Yield: 42.8 mg (49%).

IR (Nujol): ν_{max} *ca.* 3270–3650 m composite, 3086 w, 1708 w, 1623 br s, 1403 w, 1318 m, 1306 w, 1283 s, 1263 m, 1247 w, 1228 w, 1193 vw, 1168 m, 1143 s, 1116 s, 1116 s, 1095 m, 1062 w, 1041 w, 1030 m, 1020 m, 973 m, 930 w, 888 s, 857 w, 876 w, 833 vw, 828 vw, 790 m, 748 vs, 705 w, 692 w, 627 w, 609 w, 542 w, 517 m, 489 br s, 459 s cm^{-1}. Anal. calc. for $Li_2Zn_2Br_6$(**6a**)$_2$-$(MeOH)_5(H_2O)_3$ (1762.9): C 36.11, H 4.12%. Found: C 35.88, H 3.79% (the sample is slightly hygroscopic).

X-ray crystallography

The diffraction data (θ_{max} = 27.5°; data completeness ≥99.3%) were recorded with a Nonius Kappa diffractometer equipped with an APEX-II CCD detector (Bruker) and a Cryostream Cooler (Oxford Cryosystems) at 150(2) K using graphite monochromatized Mo Kα radiation (λ = 0.71073 Å) and were corrected for absorption using routines included in the diffractometer software.

The structures were solved by the direct methods (SHELXS97) and refined by full-matrix least squares routines based on F^2 (SHELXL97).[36] The non-hydrogen atoms were refined with anisotropic displacement parameters. The hydrogen atoms residing on the oxygen atoms (OH protons) in the structures of **2**·CH_3OH, **8a**, **8b**, and **9a** were identified on the difference electron density maps and refined as riding atoms with $U_{iso}(H)$ set to 1.2-times $U_{eq}(O)$. In the case of **10a**·CH_3OH, they were placed into positions suitable for the formation of hydrogen bonds and refined similarly. Hydrogen atoms residing on the carbon atoms were included in their theoretical positions and refined analogously.

Description of the crystallization experiments and a listing of relevant crystallographic data and structure refinement parameters are available in the ESI (Table S1†). Geometric data as well as all structural drawings were obtained with a recent version of the PLATON program.[37] All numerical values are rounded with respect to their estimated standard deviations (ESDs) given with one decimal. Parameters pertaining to atoms in constrained positions are presented without ESDs.

Acknowledgements

Results reported in this paper were obtained with financial support from the Czech Science Foundation (project no. 15-11571S) and the Grant Agency of Charles University in Prague (project no. 8415).

Notes and references

1 (*a*) T. J. Kealy and P. L. Pauson, *Nature*, 1951, **168**, 1039; (*b*) S. A. Miller, J. A. Tebboth and J. F. Tremaine, *J. Chem. Soc.*, 1952, 632.

2 (*a*) G. Wilkinson, M. Rosenblum, M. C. Whiting and R. B. Woodward, *J. Am. Chem. Soc.*, 1952, **74**, 2125; (*b*) E. O. Fischer and W. Pfab, *Z. Naturforsch., B: Anorg. Chem. Org. Chem. Biochem. Biophys. Biol.*, 1952, **7**, 377.

3 (*a*) *Methods of Organoelement Compounds, volume Organoiron Compounds, Ferrocene*, ed. E. G. Perevalova, M. D. Reschetova and K. I. Grandberg, Nauka, Moscow, 1983 (in Russian); (*b*) V. I. Boev, L. V. Snegur, V. N. Babin and Y. S. Nekrasov, *Usp. Khim.*, 1997, **66**, 677; (*c*) *Ferrocenes*, ed. A. Togni and T. Hayashi, VCH, Weinheim, 1995, p. 677 ff; (*d*) B. W. Rockett and G. Marr, *J. Organomet. Chem.*, 1991, **416**, 327 and previous "Annual surveys of ferrocene chemistry".

4 R. Gleiter, C. Bleiholder and F. Rominger, *Organometallics*, 2007, **26**, 4850.

5 (*a*) *Ferrocenes: Ligands, Materials and Biomolecules*, ed. P. Štěpnička, Wiley, Chichester, 2008; (*b*) R. C. J. Atkinson, V. C. Gibson and N. J. Long, *Chem. Soc. Rev.*, 2004, **33**, 313; (*c*) R. Goméz Arrayás, J. Adrio and J. C. Carretero, *Angew. Chem., Int. Ed.*, 2006, **45**, 7674.

6 A proper choice of the alkylation reagent can sometimes eliminate this problem. For an example, see: P. Štěpnička and I. Císařová, *Organometallics*, 2003, **22**, 1728.

7 M. Widhalm, U. Nettekoven and K. Mereiter, *Tetrahedron: Asymmetry*, 1999, **10**, 4369.

8 (*a*) A. Labande, J.-C. Daran, E. Manoury and R. Poli, *Eur. J. Inorg. Chem.*, 2007, 1205; (*b*) S. Gülcemal, A. Labande, J.-C. Daran, B. Çetinkaya and R. Poli, *Eur. J. Inorg. Chem.*, 2009, 1806; (*c*) A. Labande, N. Debono, A. Sournia-Saquet, J.-C. Daran and R. Poli, *Dalton Trans.*, 2013, **42**, 6531.

9 P. Štěpnička and I. Císařová, *Dalton Trans.*, 2013, **42**, 3373.

10 P. Štěpnička, M. Zábranský and I. Císařová, *ChemistryOpen*, 2012, **1**, 71.

11 For an alternative synthesis of **1**, see: M. E. Wright, *Organometallics*, 1990, **9**, 853.

12 (*a*) P. Štěpnička and T. Baše, *Inorg. Chem. Commun.*, 2001, **4**, 682; (*b*) P. Štěpnička, I. Císařová and J. Schulz, *Organometallics*, 2011, **30**, 4393; (*c*) P. Štěpnička, J. Schulz, T. Klemann, U. Siemeling and I. Císařová, *Organometallics*, 2010, **29**, 3187; (*d*) U. Siemeling, T. Klemann, C. Bruhn, J. Schulz and P. Štěpnička, *Dalton Trans.*, 2011, **40**, 4722; (*e*) P. Štěpnička and I. Císařová, *J. Organomet. Chem.*, 2012, **716**, 110.

13 V. I. Boev, *Zh. Obshch. Khim.*, 1991, **61**, 1174.

14 In addition to the betaine, the reaction of **1** with the sultone gives rise to other products, namely salt(s) with protonated amines (presumably hydrochloride), which are less polar than **2**, and some P-alkylated products (δ_P 26.7; more polar than **2**).

15 (*a*) W. Henderson, A. G. Oliver and A. J. Downard, *Polyhedron*, 1996, **15**, 1165; (*b*) Y. S. Nekrasov, R. S. Skazov, A. A. Simenel, L. V. Snegur and I. V. Kachala, *Russ. Chem. Bull.*, 2006, **55**, 1368.

16 J. K. Lindsay and C. R. Hauser, *J. Org. Chem.*, 1957, **22**, 355.

17 (*a*) M. Uher and Š. Toma, *Collect. Czech. Chem. Commun.*, 1971, **36**, 3056; (*b*) J. B. Evans and G. Marr, *J. Chem. Soc., Perkin Trans. 1*, 1972, 2502; (*c*) V. I. Boev and A. V. Dombrovskii, *Zh. Obshch. Khim.*, 1984, **54**, 1863.

18 J. H. Brownie, M. C. Baird and H. Schmider, *Organometallics*, 2007, **26**, 1433.

19 K.-S. Gan and T. S. A. Hor, in *Ferrocenes: Heterogeneous Catalysis, Organic Synthesis, Materials Science*, VCH, Weinheim, 1995, ch. 1.3, p. 19.

20 P. A. Chaloner, R. M. Harrison, P. B. Hitchcock and R. T. Pedersen, *Acta Crystallogr., Sect. C: Cryst. Struct. Commun.*, 1992, **48**, 717.

21 P. C. Healy, W. A. Loughlin, B. M. Sweeney and I. D. Jenkins, *Acta Crystallogr., Sect. E: Struct. Rep. Online*, 2002, **58**, o137. The distances and angles were calculated from coordinates deposited in the Cambridge Crystallographic Database (refcode: MIFSID).

22 F. A. M. Rudolph, A. L. Fuller, A. M. Z. Slawin, M. Bühl, R. A. Aitken and J. D. Woollins, *J. Chem. Crystallogr.*, 2010, **40**, 253.

23 C. Lichtenberg, N. S. Hillesheim, M. Elfferding, B. Oelkers and J. Sundermeyer, *Organometallics*, 2012, **31**, 4259.

24 I. R. Butler, W. R. Cullen, F. W. B. Einstein and A. C. Willis, *Organometallics*, 1985, **4**, 603.

25 J. C. J. Bart, *J. Chem. Soc. B*, 1969, 350.

26 W. E. McEwen, C. E. Sullivan and R. O. Day, *Organometallics*, 1983, **2**, 420.

27 R. G. Pearson, *J. Am. Chem. Soc.*, 1963, **85**, 3533.

28 R. H. Prince, Zinc and Cadmium, in *Comprehensive Coordination Chemistry*, ed. G. Wilkinson, R. D. Gillard and J. A. McCleverty, Pergamon, Oxford, 1987, ch. 56.1, vol. 5, pp. 925–1097.

29 The Na^+ necessary for the formation of **8a** seems to have come from the commercial $ZnBr_2$ sample, which was shown to contain 0.04 μg Na per 1 mg by atomic absorption spectrometry, or simply from the solvents and/or the glassware.

30 Increasing the chloroform-to-methanol ratio can result in a separation of the alkali metal halide (MX) from the reaction mixture (full or partial), which in turn reduces the yield of the mixed-metal complex or even fully prevents its formation. On the other hand, a low chloroform-to-methanol ratio (*i.e.*, more polar reaction mixture) can significantly reduce the yield of the desired mixed-metal complex by increasing its solubility.

31 We feel that compound **10a** need not necessarily be the only product possibly arising in the **6a**/LiBr/$ZnBr_2$ system as the reaction can, in principle, afford also other, differently solvated species.

32 See, for instance: (*a*) A. Santoro and A. D. Mighell, *Acta Crystallogr., Sect. A: Found. Crystallogr.*, 1970, **26**, 124; (*b*) V. Balashov and H. D. Ursell, *Acta Crystallogr.*, 1957, **10**, 582; (*c*) J. D. H. Donnay, *Am. Mineral.*, 1943, **28**, 507.

33 (*a*) A. Bader and E. Lindner, *Coord. Chem. Rev.*, 1991, **108**, 27; (*b*) C. S. Slone, D. A. Weinberger and C. A. Mirkin, *Prog. Inorg. Chem.*, 1999, **48**, 233.

34 The search for structurally characterised compounds combining octahedral Na(I) and tetrahedral Zn(II) sites in the Cambridge Structural Database, version 5.36 of November 2014 with updates from November 2014, resulted in 42 hits. These compounds were mostly coordination polymers featuring various O-donors. None of them contained phosphine donors or motifs similar to that encountered in **8a** and **8b**.

35 Dissolution of this by-product in dichloromethane, washing with 5% aqueous NaOH, and subsequent chromatographic purification recovered pure **1**.

36 G. M. Sheldrick, *Acta Crystallogr., Sect. A: Found. Crystallogr.*, 2008, **64**, 112.

37 A. L. Spek, *J. Appl. Crystallogr.*, 2003, **36**, 7.